Pattern of substitution affects the extractability and enzymatic deconstruction of xylan from Eucalyptus wood

Carbohydrate Polymers 353 (2025) 123246

Contents lists available at ScienceDirect

Carbohydrate Polymers

journal homepage: www.elsevier.com/locate/carbpol

Pattern of substitution affects the extractability and enzymatic deconstruction of xylan from *Eucalyptus* wood

Emilia Heinonen [a,b,*], Pramod Sivan [b], Amparo Jiménez-Quero [d], Mikael E. Lindström [c], Jakob Wohlert [a,c], Gunnar Henriksson [a,c], Francisco Vilaplana [a,b,*]

[a] Wallenberg Wood Science Center, KTH Royal Institute of Technology, Teknikringen 56-58, 10044 Stockholm, Sweden
[b] Division of Glycoscience, Department of Chemistry, KTH Royal Institute of Technology, AlbaNova University Centre, Roslagstullsbacken 21, 10691 Stockholm, Sweden
[c] Department of Fibre and Polymer Technology, KTH Royal Institute of Technology, Teknikringen 56-58, 10044 Stockholm, Sweden
[d] Division of Industrial Biotechnology, Department of Life Sciences, Chalmers University of Technology, Kemigården 1, 41296 Gothenburg, Sweden

ARTICLE INFO

Keywords:
Eucalyptus
Xylan
Glucuronidation
Acetylation
Galactosylation
Recalcitrance

ABSTRACT

Glucuronoxylan is the main hemicellulose in the secondary cell wall of angiosperms. Elucidating its molecular structure provides a basis for more accurate plant cell wall models and the utilization of xylan in biorefinery processes. Here, we investigated the spacing of acetyl, glucuronopyranosyl and galactopyranosyl substitutions on *Eucalyptus* glucuronoxylan using sequential extraction combined with enzymatic hydrolysis and mass spectrometry. We found that the acetyl groups are preferentially spaced with an even pattern and that consecutive acetylation is present as a minor motif. Distinct odd and even patterns of glucuronidation with tight and sparse spacing were observed. Furthermore, the occurrence of consecutive glucuronidation is reported, which adds to the growing body of evidence that this motif is not only present in gymnosperms but also in angiosperms. In addition, the presence of terminal galactopyranosyl units, which can be released by β-galactosidase, altered the digestibility of the glucuronoxylan by GH30 and GH10 xylanase and appeared to be clustered within the polymeric backbone. These findings increase our understanding of the complex structure of glucuronoxylans and its effect on the extractability and biological degradation of *Eucalyptus* wood.

1. Introduction

Eucalyptus species are today the most important pulp woods due to their fast life cycle, high cellulose content and high fibre quality (Sixta, 2006). As with any other woody biomass, the utilization of the hemicelluloses and lignin fractions for other than energy is hindered by their structural complexity making the cell wall recalcitrant and extraction processes costly. Given that the hemicelluloses and lignin account for 50–60 % of the lignocellulosic biomass (Timell, 1964, 1965), it is hardly possible to increase the sustainability of bio-based processes without using these fractions for higher value applications. Therefore, improvements in the fractionation processes as well as the characterization of hemicelluloses and lignin are needed.

Eucalyptus wood contains 41–51 % of cellulose, 19–28 % lignin, 15–23 % of glucuronoxylan (GX) and 1–4 % of glucomannan (Carvalho, 2015; Willför et al., 2005). Hardwood lignin is composed of syringyl (S), guaiacyl (G) and to a minor extent p-hydroxy-phenyl (H) units linked together primarily by β-O-4 linkages. Glucomannan is built of 1 → 4 linked D-manno- and glucopyranosyl (Man*p*, Glc*p*) residues in a ratio of 1–2:1 whereas xylan has backbone of 1 → 4 linked D-xylopyranosyl (Xyl*p*) units, that are occasionally acetylated at the O2 and/or O3 positions and substituted by 4-*O*-methyl-α-(1 → 2)-D-glucuronic acid (MeGlcpA) (Fig. 1A) (Sjöström, 1993). *Eucalyptus* xylan is not interesting only because of its potential commercial value, but because of its peculiar molecular structure. Shatalov et al. (1999) were the first to show that an extract of xylan contained an unusually high amount of galactose that was not removed by purification steps. Linkage and NMR analyses confirmed that the xylan carries galactopyranosyl (Gal*p*) residues 1 → 2 linked to the MeGlcpA.

Spacing of the substitutions is critical for the interaction of xylan with cellulose microfibrils enabling normal plant growth (Grantham et al., 2017). In that regard, both acetyl and MeGlcpA have been shown to preferentially be evenly spaced (Busse-Wicher et al., 2014; Chong et al., 2014; Grantham et al., 2017), and that the even acetylation

* Corresponding authors at: Wallenberg Wood Science Center, KTH Royal Institute of Technology, Teknikringen 56-58, 10044 Stockholm, Sweden.
E-mail addresses: sehei@kth.se (E. Heinonen), psivan@kth.se (P. Sivan), amparo@chalmers.se (A. Jiménez-Quero), mil@kth.se (M.E. Lindström), jacke@kth.se (J. Wohlert), ghenrik@kth.se (G. Henriksson), franvila@kth.se (F. Vilaplana).

https://doi.org/10.1016/j.carbpol.2025.123246
Received 4 November 2024; Received in revised form 31 December 2024; Accepted 6 January 2025
Available online 10 January 2025

facilitates correct glucuronosyltransferase function and interaction of xylan with cellulose in the cell wall (Grantham et al., 2017). On the other hand, minor domains of consecutive glucuronidation and acetylation have been proposed to link with lignin (Sivan et al., 2024). To that end, sequential extractions on birch and spruce have shown that longer extraction times yield xylan with tighter MeGlcpA spacing (Martínez-Abad et al., 2018; Martínez-Abad et al., 2020). Here we are interested in investigating the supramolecular structure of *Eucalyptus* wood xylan and its significance in biomass recalcitrance.

Eucalyptus xylan has traditionally been extracted by one-step alkaline, water or DMSO extraction from pulp (Lisboa et al., 2005), black liquor (Lisboa et al., 2005; Magaton et al., 2012) and wood or holocellulose (Carvalho, 2015; Gullón et al., 2011; Kabel, 2002; Shatalov et al., 1999; Togashi et al., 2009). Alkaline extraction gives a high yield but results in deacetylation of the xylan. DMSO is an efficient solvent, albeit not for large industrial-scale processing of wood and requires prior delignification, which in the research context prevents evaluation of the xylan recalcitrance. Previous water extractions were performed at low temperatures with low yield as a result (Kabel, 2002) or at high temperature and unbuffered conditions which led to partial deacetylation and depolymerization (Alonso et al., 2002; Garrote et al., 2001; Gullón et al., 2011; Kabel et al., 2002). Extraction of polymeric xylan directly from wood in high yield, so in representative quantity, is desired. Recently, sequential subcritical water extraction (SWE) in buffered conditions has been developed for this purpose in different softwood and hardwood species (Martínez-Abad et al., 2018, 2020; Sivan et al., 2023). The SWE process helps to preserve labile functional groups such as the acetylation while being able to extract xylan with a high degree of polymerization (DP) (Martínez-Abad et al., 2018). The SWE extraction does not hinder the further utilization of the wood, on the contrary, some properties such as saccharification are superior compared to untreated wood (Sivan et al., 2023).

This work aims to improve our fundamental understanding of the structure-recalcitrance relationship of *Eucalyptus* xylan in terms of the acetyl, MeGlcpA and Galp substitutions. Obtaining a higher yield of polymeric xylan with their side chain functionalities by sequential extraction and careful characterization of the fractions will help to decipher the molecular structure of *Eucalyptus* xylan and its effect on the extractability.

To that end, we implemented an integrated strategy combining the sequential subcritical water (SWE) and alkaline extraction methods that are well established for wood fractionation (Martínez-Abad et al., 2018; Scott, 1989; Timell, 1961; Willför et al., 2005). The extractability of the hemicelluloses was monitored by comparing the monosaccharide composition, the molecular weight distribution and the degree of acetylation in the sequential extracts. Oligomeric mass profiling (OLIMP) was used for elucidating the substitution pattern of the xylan. More specifically, digestion of GX using specific xylanases followed by glycan sequencing by MS/MS was implemented to unravel the molecular architecture of structural motifs such as galactose substitution which is unique to Eucalyptus GX. Together with the calculated mass balance we can evaluate how the molecular architecture of the *Eucalyptus* hemicelluloses is related to their extractability and how it compares to that of other hardwoods.

2. Material and methods

2.1. Extraction and purification of hemicelluloses

2.1.1. Preprocessing

Eucalyptus chips were milled to powder (40 um mesh size), purified from extractives by Soxhlet extraction using acetone and air dried.

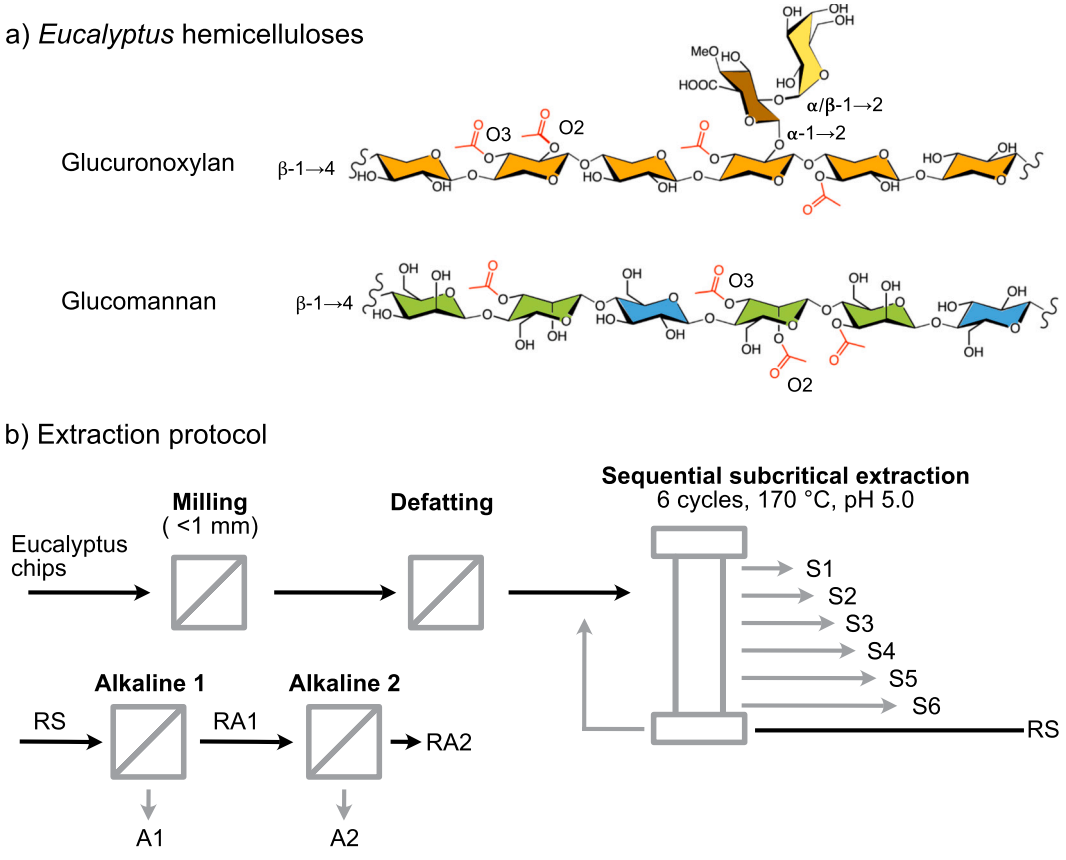

Fig. 1. a) Hemicelluloses in *Eucalyptus*. Acetylated glucuronoxylan with *Eucalyptus* unique MeGlcpA-Galp substitution and glucomannan. b) Extraction protocol.

2.1.2. Subcritical water extraction (SWE)

For the SWE of *Eucalyptus* xylan, we used the conditions previously optimized for birch without prior delignification (Martínez-Abad et al., 2018). In short, 5 g of milled wood was extracted in triplicate at pH 5.0 (0.2 M sodium formate buffer), 170 °C and 100 bar using an accelerated solvent extractor (ASE-300, Dionex, USA). The extraction proceeded in 6 cycles with residence times of 5, 15, 20, 20, 60 and 120 min. The extract was automatically recovered after each cycle and the sample vessel was filled with fresh buffer. Salts and low molecular weight compounds were removed by dialysis using Spectra/Por3 membranes (MWCO 3.5 kDa, Spectrum, USA) after which the extracts were freeze-dried and weighed before further analyses.

2.1.3. Alkaline extractions

The residue from the subcritical water extraction (SWE residue) was subjected to alkaline extraction in duplicate as described by (Timell, 1961). The dry residue was mixed in 24 % KOH in a solid-to-liquid ratio 1:10, purged with N_2, sealed and stirred for 24 h at room temperature. The extract was filtered through a 60 um wire, mixed with HAc and 96 % EtOH in the ratio of 1:0.4:4 (v:v:v, extract, HAc and EtOH), and placed in 4 °C overnight. The precipitated material was collected by centrifugation and washing several times with 80 % EtOH. After the final washing, the extracts were dispersed in MilliQ-H_2O and freeze-dried. The residue (KOH residue) was washed with DI-H_2O until the pH of the washings was below 8, and freeze-dried. The second alkaline step was performed similarly in duplicate, except 17.5 % NaOH +4 % H_3BO_3 was used as a solvent to enhance the glucomannan extraction (Timell, 1961). Furthermore, the solid-to-liquid ratio was decreased to 1:15 for sufficient mixing. The second alkaline step yielded an extract and the final residue (NaOH residue).

2.2. Chemical characterization of the extracts and the residues

2.2.1. Monosaccharide composition

The cellulose-rich starting material and residues from each extraction step were subjected to sulfuric acid hydrolysis. In brief, 200 mg of dry material was weighted in triplicate into a glass bottle and 3 mL 72 % (*w*/w) H_2SO_4 was added. The bottles were placed under vacuum, stirred after 1 h and allowed to stand under the vacuum for 20 more minutes. Then 84 mL of MilliQ water was added and the bottles were closed tightly. The samples were autoclaved at 125 °C for 60 min. The hydrolyzed samples were filtered through dried and weighted glass fibre filters (Whatman™ GF/A 47 mm), and the filters were washed with 2x5mL boiling MilliQ water. The filtrate was transferred to a volumetric flask of 100 mL and MilliQ water was added up to the mark. The filtrate was then diluted 10 or 20 times for quantification of the released monosaccharides or the acid-soluble lignin, respectively. The filter cake was rinsed with 100 mL boiling water, 100 mL cold water and dried at 105 °C to determine the amount of acid-insoluble (Klason) lignin.

The monosaccharide composition of the extracts was analyzed by acid-methanolysis. In brief, 1 mg of the sample was weighed in a glass vial in triplicate. 1 mL 2 M HCl in MeOH was added, the vials were flushed with Argon and the lids were sealed with PTFE tape. Samples were heated for 5 h at 100 °C. Then, the samples were neutralized by pyridine, cooled down to room temperature and dried under N_2. Next, 1 mL 2 M TFA was added and the samples were heated for 1 h at 120 °C. Finally, the samples were dried under air flow, redissolved in MilliQ-water, diluted 10 times and filtered through 0.2 μm Chromacol syringe filters (17-SF-02(N), Thermo Fisher Scientific). Monosaccharides from both sulfuric acid hydrolysis and methanolysis were quantified by high-performance anion exchange chromatography coupled to a pulsed amperometric detector (HPAEC-PAD, ICS-3000 Dionex) as described previously (McKee et al., 2016). CarboPac PA1 column (4x250mm Dionex) was calibrated by running monosaccharide standards at 0.005, 0.01, 0.02, 0.05 and 0.1 g/L.

2.2.2. Lignin content

The Lignin content of the extractive-free wood material and the residues was determined as the sum of the acid-soluble and insoluble lignin after the sulfuric acid hydrolysis (triplicate hydrolyses, see monosaccharide composition method). The former was quantified from the filtered solution using a UV-spectrophotometer (Shimadzu UV-2550) and calculated using the following equation:

$$ASL\% = 100 * \frac{A * V * f}{\varepsilon * l * M} - 0.2 \quad (1)$$

where A = absorbance at 205 nm (average of five scans), V = volume of hydrolyzed sample in L, f = dilution factor, l = cuvette length in cm, M = sample dry weight in g, ε=absorbtivity 113 [g cm]$^{-1}$ for hardwoods. Lignin content of the hemicellulose-rich extracts was estimated based on the total monosaccharide content.

2.2.3. Molar mass distributions

The molar mass of the extracts was determined by size exclusion chromatography coupled to a UV and refractive index detectors (SECurity 1260, Polymer Standard Services, Mainz, Germany) and to Multi-angle laser light scattering detectors (Polymer Standard Services, Mainz, Germany). The UV detector was set to 280 nm. The samples were dissolved in 2 mg/mL (single sample) in 100 mM $NaNO_3$ with 10 mM NaN_3 at 40 °C, and filtered through 0.2 μm Chromacol Nylon syringe filters (Thermo Scientific™). 100 μl sample was injected and the separation was carried through SUPREMA Analytical columns of 30 Å and 2 × 1000 Å (Polymer Standard Services, Mainz, Germany) at a flow rate of 1.0 mL/min and 40 °C. The columns were calibrated using pullulan standards between 345 and 708,000 Da (Polymer Standard Services, Mainz, Germany).

The molecular weight distribution of the extracts before and after the digestions with glucuronoxylanase (GH30) was determined using HPLC coupled to a UV (Dionex-Thermofisher Ultimate 3000, USA) and a refractive index detector (Waters 2412) running on 10 mM NaOH. 40 μl sample was injected and the separation was carried through SUPREMA Analytical columns of 30 and 2 × 1000 Å (Polymer Standard Services, Mainz, Germany) at a flow rate of 1.0 mL/min and 40 °C. The columns were calibrated as described above and 30 °C post-column cooling was applied before the detectors.

2.2.4. Acetyl content

The acetyl content was determined by saponification of the acetyl groups and subsequent quantification of the released acetic acid. Shortly, about 5 mg of the sample was weighed in triplicate and incubated overnight in 0.8 M NaOH at 60 °C with constant mixing. Samples were then neutralized with 37 % HCl and passed through 0.2 μm Chromacol syringe filters (17-SF-02(N), Thermo Fisher Scientific). 50 μl of the sample was injected in HPLC coupled to a UV-detector (HPLC-UV Dionex-Thermofisher Ultimate 3000, USA) and separated in a Rezex ROA-organic acid column (300 × 7.8 mm, Phenomenex, USA) at 50 °C in a 2.5 mM H_2SO_4 at 0.5 mL/min. The acetic acid was detected by UV-absorbance at 210 nm and the concentration was calculated based on a linearly fitted standard curve of 6 acetic acid standards (1 mM - 60 mM). Propionic acid was used as an internal standard.

2.3. Enzymatic profiling and oligomeric sequencing of glucuronoxylan

2.3.1. Enzymatic digestion and oligomeric analysis by HPAEC-PAD

Before the enzymatic hydrolysis, an aliquot of each extract was chemically deacetylated as described previously (Martínez-Abad et al., 2018). Both deacetylated and intact extracts were dissolved at 2 mg/mL by mixing in 0.02 M sodium acetate buffer (pH 5.5) at 60 °C for 24 h, cooled down to 37 °C and incubated for 24 h with GH30 *endo*-β-(1 → 4)-glucuronoxylanase (10 U/mL) (kindly provided by Prof. James F. Preston, University of Florida). The same conditions were used for

incubations with α and β-galactosidase (GH36 and GH35, Megazyme). For incubations with GH10 xylanase (Megazyme) 0.1 M sodium acetate buffer at pH 5.0 was used and the samples were incubated at 60 °C with enzyme (10 U/mL). The enzymes were denatured at 95 °C for 10 min and centrifuged if a visible precipitate was observed (alkali extracts). Then an aliquot was taken for SEC analysis and the rest of the sample was filtered through a 10 k centrifugal filter (Amicon® Ultra-0.5) and kept at −20 °C. All the incubations were performed in duplicates and a positive blank (extract without the enzyme) was included to account for oligosaccharides present before the enzymatic digestion. The released oligosaccharides were separated and detected by HPAEC-PAD as described elsewhere (McKee et al., 2016).

2.3.2. Oligomeric mass profiling (OLIMP)

For direct oligomeric mass profiling the samples were diluted in 50 % acetonitrile and 0.1 % formic acid. OLIMP was performed using an LC system coupled to an electrospray ionization mass spectrometry (ESI-MS, Synapt G2, Waters Corporation, Milford, MA, USA) in positive ion mode. Samples were passed through a ZORBAX Eclipse Plus C18 column (1.8 μm, 2.1 × 50 mm, Agilent Technologies, Santa Clara, USA) for automation. The capillary and cone voltage were set to 3 kV and 60 V, respectively and the oligosaccharides were detected as $[M + Na]^+$ adducts. The relative abundance of oligosaccharides represents the average of duplicate incubations. First, the ion counts from the blank (extract without the enzyme) were deducted from each sample. Then, the average ion count of the duplicates was calculated. Finally, the ion counts were normalized to the sum of all the ion counts, giving the relative abundance of each ion.

2.3.3. Derivatization and structural determination by LC-ESI-MS/MS

The GH10 digested oligosaccharides were filtered through 10 k centrifugal filter (Amicon® Ultra-0.5) and labelled by reductive amination with anthranilic acid (AA) in duplicate. Furthermore, the blanks from the enzymatic digestions were also derivatized. 200 μg of sample was dissolved in 250 μl of MilliQ. 125 μl MeOH and 75 μl HAc were added and the samples were incubated at 40 °C for 30 min after the addition of 2.27 μL of 1 M AA in MeOH, and further 45 min after the addition of 3.8 μL of 1 M picoline borane in MeOH:HAc (*v*/v, 50:50). The samples were dried under a stream of air and dissolved in 10 % acetonitrile in water. The labelled oligosaccharides were separated through ACQUITY UPLC HSS T3 column (150 × 2.1 mm, Waters, USA) at a flow rate of 0.3 mL/min with a gradient of acetonitrile +0.1 % (*v*/v) formic acid. MS analysis was performed in positive ion mode with capillary and cone voltage set to 3 kV and 60 V, respectively. MS/MS was performed by selecting the ion of interest through single ion monitoring (SIM) and subjecting it to collision-induced dissociation (CID) using argon as collision gas, at a ramped voltage 35–85 V. The assignment of the mass and the fragmentation spectra was performed using ChemDraw (PerkinElmer, Waltham, Massachusetts, USA). Fragments were assigned according to the nomenclature proposed by (Domon & Costello, 1988). The naming of the proposed structures is based on the nomenclature by (Fauré et al., 2009).

3. Results and discussion

3.1. Sequential subcritical water extraction of hemicelluloses yields different matrix polysaccharide populations from Eucalyptus wood

Hemicelluloses from milled and defatted *Eucalyptus* wood chips were extracted using a sequential approach (Fig. 1B). First, we applied similar subcritical water cycles that were developed for the extraction of hemicelluloses from birch wood without previous delignification (Martínez-Abad et al., 2018). In short, a buffer at pH 5.0 minimizes the deacetylation of the xylan and a temperature of 170 °C is suitable for extracting polymeric xylan from hardwoods. At lower temperatures, the yield is minimal whereas at higher temperatures extensive depolymerization occurs (Leppänen et al., 2010). Because only a part of the hemicelluloses were solubilized with subcritical water, the SWE residue was further extracted with aqueous alkali. In that regard, the first alkaline step with KOH targeted the recalcitrant xylan, while the second alkaline step with NaOH and boric acid the recalcitrant glucomannan. (Mian & Timell, 1960).

The mass balances and the average composition of the wood, extracts and residues are shown in Fig. 2 and Table 1. When SWE and the two alkaline steps are summarized, 21 % of the solids were extracted, 49 % remained in the final residue and 30 % of the solids were lost during the extraction steps (Fig. 2B). The residue RA2 consists mainly of cellulose and lignin (Fig. 2A). We assigned the loss of material first to the removal of low molecular weight compounds by the dialysis of the SWE extracts and later to the separation of ethanol-soluble compounds during the precipitation of the alkaline extracts. The extraction yield of the SWE was 12.5 % (total extraction time of 240 min). Previously yields of 11–12 %, 24 % and 7.7 % have been obtained from aspen, birch and spruce with total extraction times of 120, 240 and 320 min (Martínez-Abad et al., 2018, 2020; Sivan et al., 2023). Because cellulose remains intact during the SWE process (Martínez-Abad et al., 2018), the lower yield of solids from *Eucalyptus* compared to the other hardwoods (aspen and birch) can be ascribed to its high cellulose content (Willför et al., 2005).

The monosaccharide composition of the subcritical water extracts (S1-S6) shows a typical pattern previously observed with birch (Martínez-Abad et al., 2018) and aspen (Sivan et al., 2023). The first extracts contain mainly water-soluble lignin and easily soluble polysaccharides such as pectins, starch and glucomannan (Fig. 2A). Here, glucose-rich polymers (starch, callose) are preferably extracted in the first cycle, whereas the highest amount of rhamnose, galactose and galacturonic acid is detected in the S2 fraction. Therefore, the S2 is enriched in pectic rhamnogalacturonan that carries arabinose and galactose side chains. The galacturonic acid content of the extracts decreases after the S2 cycle below the detection limit at S6, which further shows the preferential extraction of pectins at short residence times.

As expected, the xylan content increases with the extraction time and the S3-S6 fractions contain mostly xylan. In S5-S6 xylan accounts for over 90 % of the carbohydrates. The cumulative yield of xylose (Fig. 2B) highlights the efficiency of the SWE protocol used since 42 % of the xylan is recovered after dialysis. Despite the high SWE yield 43 % of the xylan remains in the wood. For birch, the same protocol left 30 % of the xylan in the residue (Martínez-Abad et al., 2018), which shows that *Eucalyptus* xylan is more resistant to subcritical water extraction and prompted us to continue the extraction with more powerful solvents. The first alkaline step with 24 % KOH removed most of the recalcitrant xylan, which accounted for 24 % of the xylan in wood. A total of 13 % of the wood xylan was lost and 6 % remained in the RA1 residue. The monosaccharide analysis showed that the A1 xylan has very high purity as it contains 97 % carbohydrates of which xylan accounts for 91.5 %. The subsequent NaOH step recovered 2.5 % of the xylan, leaving only 3.9 % in the final residue. This is in line with previous studies that have shown that the complete removal of hemicelluloses from wood is practically impossible without causing partial cellulose degradation (Timell, 1964). Combined recovery of *Eucalyptus* xylan from SWE, A1 and A2 is 68 %. Previously, typical yields have ranged from 7 to 27 % depending on the extraction method (Carvalho, 2015; Gullón et al., 2011; Kabel, 2002; Lisboa et al., 2005; Magaton et al., 2012; Shatalov et al., 1999; Togashi et al., 2009). Two studies obtained high yields of 43 and 46 % by alkaline extraction of pulp (Corradini et al., 2018) or DMSO extraction of holocellulose (Evtuguin et al., 2003), while our sequential extraction approach provided high xylan recovery without the need for prior delignification of the wood.

The molar mass of the xylan-rich fractions from SWE is 13–21 kDa, which is typical for water-extracted xylans (Martínez-Abad et al., 2018; Sivan et al., 2023), and in line with previous results on Eucalyptus, where the molar mass was found to vary between 14 and 55 kDa

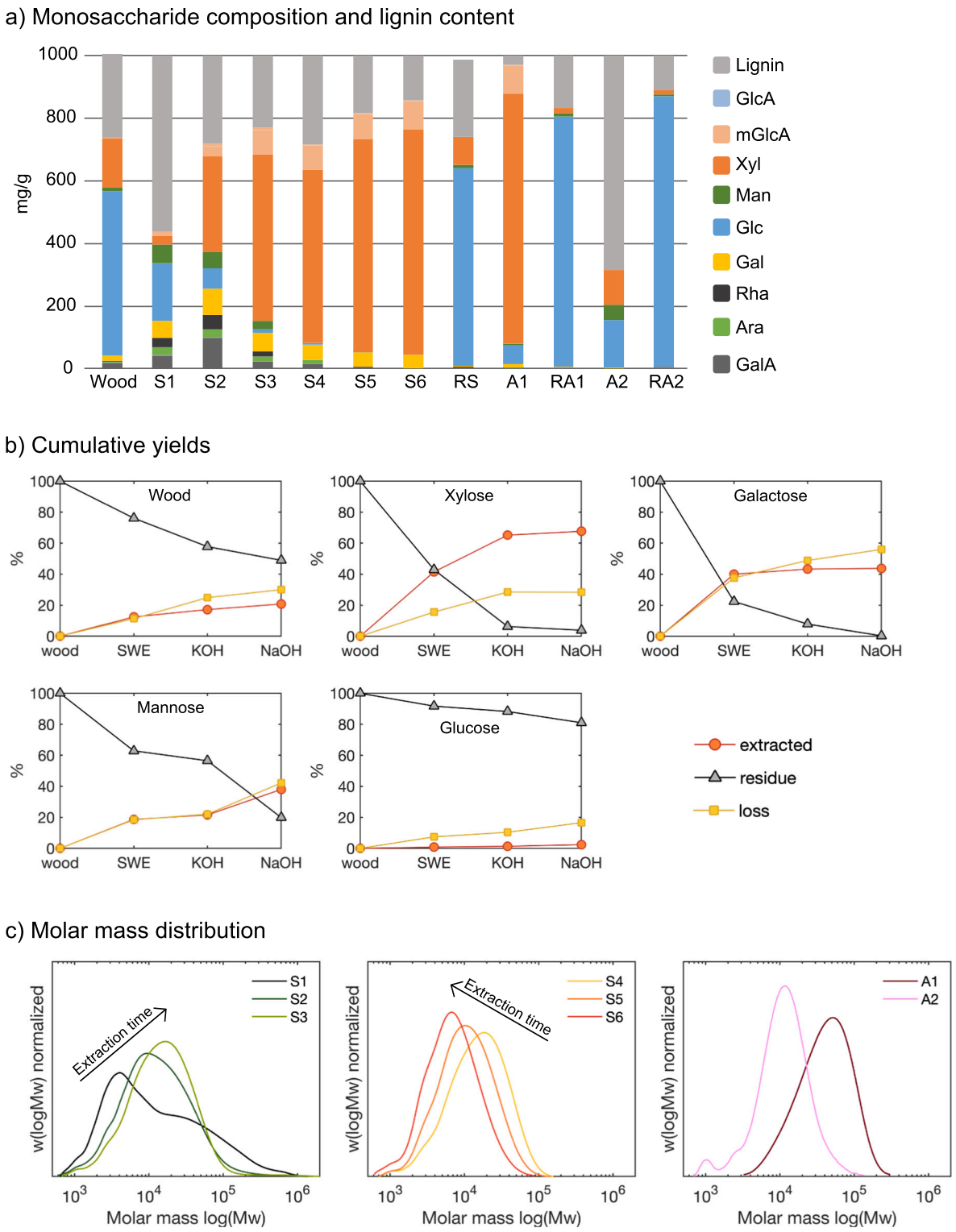

Fig. 2. A) Monosaccharide composition. Wood and solid residues after sulfuric acid hydrolysis. Lignin content as the sum of acid-insoluble and soluble fractions. Extracts by acid-methanolysis and the lignin content estimated from the total sugar content. B) Yield of xylose, galactose, mannose and glucose. SWE as the sum of the subcritical water extraction step C) Molar mass distributions of the extracts from HPLC-SEC, calibration with pullulan standards.

(Carvalho, 2015; Evtuguin et al., 2003; Magaton et al., 2012; Shatalov et al., 1999). Here the polydispersity decreases with the SWE extraction time (Fig. 2C), which agrees with the increasing purity (in terms of xylan content). The multimodal distribution of the S1 extract shows that different polymeric populations are present. The main peak below 10 kDa can be attributed to glucomannan and low molar mass xylan whereas the shoulder reaching up to 1000 kDa is a typical sign of starch and other easily extractable high molecular weight plant cell wall polysaccharides.

A closer investigation of the molecular features of xylan reveals some structural differences between the extracts. The MeGlcA to xylose ratio is 0.07–0.10 in the SWE and KOH extracts (S1-S6, A1), which is in the

Table 1
Composition of *Eucalyptus* wood, subcritical water extracts (S1-S6), residue (RS), KOH extract (A1) and residue (RA1), NaOH extract (A2) and residue (RA2).

		Subcritical water							Alkaline			
Sample	Wood	S1	S2	S3	S4	S5	S6	RS	A1	RA1	A2	RA2
Extraction time[1]	NA	5	15	20	20	60	120	NA	24	NA	24	NA
Solid yield (%)	100	1.8	1.1	1.5	1.7	4.1	2.3	76.1	4.7	57.8	3.6	49.0
Xylose yield (%)[2]	100	0.3	2.2	5.0	5.8	17.5	10.6	42.9	23.7	6.3	2.5	3.9
Mannose yield (%)[2]	100	9.7	5.2	3.8	0.0	0.0	0.0	62.9	2.9	56.5	16.5	19.8
Galactose yield (%)[2]	100	5.9	5.8	5.5	5.1	11.4	6.3	22.4	3.3	7.9	0.5	0.3
Carbohydrates (mg/g)	737	437	719	769	718	817	858	740	970	829	317	882
Xylan (%)[3]	21.5	7.3	46.9	79.1	87.9	93.0	94.5	12.1	91.5	2.1	35.1	1.4
Mannose (%)[3]	1.5	13.8	7.1	3.6	0.0	0.0	0.0	1.2	1.3	1.3	15.9	0.5
Galactose(%)[3]	2.2	12.2	11.6	7.7	6.7	5.5	5.1	0.6	1.2	0.3	0.8	0.0
MeGlcA:Xyl	ND	0.10	0.07	0.07	0.07	0.08	0.09	ND	0.08	ND	0.01	ND
Gal:MeGlcA	ND	–	3.1	1.3	1.0	0.65	0.59	ND	0.15	ND	0	ND
Lignin (mg/g)[4]	272	563	282	256	302	182	144	248	30	166	684	173
DsAc[5]	ND	nc	1.68	1.31	1.08	0.54	0.63	ND	0	ND	0	ND
Mn (kDa)[6]	NA	11.1	7.3	8.9	9.6	7.2	4.9	NA	28.9	NA	7.6	NA
Mw (kDa)[6]	NA	41.0	23.1	13.1	21.0	14.4	9.4	NA	52.7	NA	14.6	NA

[1] Extraction time of S1-S6 in minutes, A1-A2 in hours.
[2] Calculated from the mass balance and the monosaccharide composition.
[3] Percentage of the total carbohydrates.
[4] Acid soluble and insoluble lignin of wood and residues. For extracts estimated from the carbohydrate analysis.
[5] Degree of acetylation by saponification, corrected by xylose content (calculated as in Xu et al. (2010). Not calculated for the S1.
[6] Number and weight average molecular mass from HPLC-SEC.

range with previous studies that found ratios of 0.05–0.16 (Carvalho, 2015; Evtuguin et al., 2003; Gomes et al., 2020; Kabel, 2002; Kabel et al., 2002; Shatalov et al., 1999). Sequential extraction of birch and aspen showed a slight increase of the MeGlcA:Xyl in the xylan-rich fractions, 0.06–0.09 and 0.14–0.17, respectively (Martínez-Abad et al., 2018; Sivan et al., 2023). Here the change between S2 and S6 is in the same range as in the birch xylan. The small change on the MeGlcA:Xyl indicates that the *degree* of glucuronidation has only a moderate effect on recalcitrance to the extraction of hardwood xylan by subcritical water.

The presence of galactose in *Eucalyptus* xylan is specifically interesting, as it is covalently linked to the MeGlcpA substitutions on the xylan backbone (Shatalov et al., 1999). Here the time evolution of galactose content shows that a significant amount of galactose is present in all the SWE fractions (S1-S6). This is contrary to SWE of birch and aspen where galactose is mainly found in the first fraction, together with arabinose, rhamnose and galacturonic acid (Martínez-Abad et al., 2018; Sivan et al., 2023), evidently originating from the β-galactan side chains of pectin. The high galactose content of xylan-rich fractions S3-S6 agrees with the presence of covalently linked galactose. Unfortunately, almost half of the galactose removed during the SWE is lost by cleavage and subsequent removal by dialysis (Fig. 2B). This is not surprising considering that part of the galactose side groups can be easily cleaved in rather mild extraction conditions (Leppänen et al., 2010). The labile nature of the galactose is further emphasized during the subsequent alkaline steps in which most of the remaining galactose is lost leaving the residue practically free from galactose (0.3 % of the galactose in wood). Due to the high galactose content of the extracts, we calculated the molar ratio of Gal:MeGlcA. Previous studies have reported ratios of 0.13–0.30 in *Eucalyptus* xylan (Carvalho, 2015; Evtuguin et al., 2003; Kabel, 2002; Shatalov et al., 1999). The presence of arabinose, rhamnose and galacturonic acid in the S1-S4 extracts and the Gal:MeGlcA ratio over 1.0 indicates that a large part of the galactose originates from pectin. Here a large difference is observed between the alkali and water-extracted xylans in that the A1, S5 and S6 have Gal:MeGlcA of 0.15, 0.65 and 0.59.

Another important molecular feature of the xylan is acetylation. We observed a decrease in the DsAc from 1.68 to 0.54 between the S1 and S5. Other studies on *Eucalyptus* have reported DsAc of 0.39–0.61 (Carvalho, 2015; Evtuguin et al., 2003; Kabel, 2002), which confirms that this SWE protocol is efficient in hindering deacetylation of the xylan. The DsAc of the S1 and S2 is probably overestimated because we assigned all the acetyl groups to the xylan, while these extracts contain a significant amount of glucomannan. The A1 and A2 xylans were deacetylated already during the extraction so it was not possible to estimate the DsAc of the recalcitrant xylan.

In addition to glucuronoxylan, all hardwoods contain 1–4 % glucomannan (Sjöström, 1993; Willför et al., 2005). Because of its low abundance, it is not a significant source of polysaccharide for industrial applications but has some very interesting features from the plant cell wall chemistry point of view. One of those features is its interaction with the other cell wall polymers. Martínez-Abad et al. (2018) suggested that the hardwood glucomannan is easily extractable, possibly due to higher mobility and lesser association with cellulose and lignin. This is true for the first fraction of glucomannan. However, monosaccharide analyses and yields confirm that 55, 68 and 63 % of the mannose from birch (Martínez-Abad et al., 2018), aspen (Sivan et al., 2023) and here from *Eucalyptus* remains in the residue after the SWE. We were able to extract some of that recalcitrant glucomannan in the second alkaline step with NaOH and sodium borate (Fig. 2B). Repeated NaOH borate extraction could help to release more glucomannan, although it was not attempted here as complete removal is very difficult and usually leads to degradation of the cellulose (Mian & Timell, 1960). After all the extraction cycles there was 12.5 mg/g xylose and 4.5 mg/g mannose left in the residue, which accounted for 3.9 % and 19.8 % of the initial amount of the respective sugars in wood. In this regard, the glucomannan is similar in hardwoods and softwoods. It is well known that softwood glucomannan has easily extractable and more recalcitrant fractions, which differ by the galactose content (Sjöström, 1993). As far as we know, hardwood glucomannan is a linear polymer and not galactosylated. However, structural variation could occur on the backbone. Earlier it has been shown that an easily extractable fraction of birch glucomannan (2 % of mannose from wood) has twice as much mannose than glucose (Man:Glc 2.1–2.4:1) (Teleman et al., 2003), whereas a larger glucomannan population extracted from delignified and KOH extracted birch by NaOH had an equimolar ratio (1:1) (Mian & Timell, 1960). In softwoods, higher glucose content has been proposed to facilitate interactions with the cellulose surfaces (Martínez-Abad et al., 2020).

3.2. Eucalyptus xylan contains a large diversity of glucuronidation and acetylation patterns

The oligomeric profiles of Eucalyptus xylan during the sequential extraction were studied by enzymatic hydrolysis of the extracts followed by ESI-MS. In this work we used two xylanases that cleave β-(1 → 4)-xylosidic linkages. GH10-β-xylanases primarily hydrolyse unsubstituted parts of the xylan backbone but can tolerate MeGlcpA and Araf substitutions to some extent in the −1 position (Linares-Pasten et al., 2017). On the other hand, GH30-β-glucuronoxylanases are highly specific towards the MeGlcpA substituted xylan backbone and require a MeGlcpA in the −2 position for hydrolytic cleavage (Hurlbert & Preston, 2001).

Figs. 3 and 4 show xylo-oligosaccharides (XOs) released from the SWE extracts S2, S4 and S6, and the alkali extract A1 by GH30 as detected by HPAEC-PAD and ESI-MS, respectively. These samples reveal the major trends in xylan substitution. The HPAEC-PAD and ESI-MS results of the S1, S3, S5 and A1 samples can be found in the supplementary material (Figs. S4-S7).

The HPAEC-PAD separates the XOs so that the neutral XOs elute between 0 and 15 min, whereas the glucuronated xylo-oligosaccharides (UXOs) elute after 15 min. The signal intensities agree with the monosaccharide analysis in that the highest intensities of UXOs are observed in the xylan-rich extracts S3-S6. Unfortunately, the lack of UXO standards prevents quantitative analysis of the acidic xylo-oligosaccharides from the HPAEC-PAD. However, a series of neutral XOs were generated by GH30, which agrees with the observation that GH30 recognizes acetylation, even if the primary activity is towards 4-O-MeGlc-Xylan (Busse-Wicher et al., 2014). This is further confirmed when comparing the profiles of acetylated and deacetylated extracts (coloured and black lines, Fig. 3a) since the digestions of deacetylated samples yield a smaller amount of neutral XOs. On the other hand, the improved digestion of the deacetylated SWE extracts as shown by the HPLC-SEC profiles (Fig. S3) indicates also that a very high degree of acetylation may hinder GH30. In the case of the alkaline extracts, the issue was that they were only partially soluble (Fig. S2), although the soluble part was mostly hydrolyzed.

3.2.1. Preference for even glucuronidation in Eucalyptus GX

Fig. 4a shows the spectra of extracts that were first chemically deacetylated (alkali extract A1) and then digested by GH30. Both even and odd spacing of MeGlcpA is observed in all samples. The main UXO of the S1-S5 is X_5U while in S6 (last SWE cycle) X_3U and X_5U are equally abundant. Previously X_5U has been reported on birch (Martínez-Abad et al., 2018) and aspen (Sivan et al., 2024). Here the SWE and the subsequent alkaline extractions show that the relationship between the recalcitrance and the xylan structure is not straightforward. The easily extractable (S1-S3) xylans from the SWE and the alkali extractable (A2-A1) xylans are relatively similar concerning the glucuronidation with larger signals from $X_{8\text{-}12}U$ oligosaccharides. Instead, the SWE xylan from later cycles (S5-S6) has more tightly spaced MeGlcpA. The difference between the S1-S3 and A1-A2 may be with the acetylation, which unfortunately was lost for the A1-A2 in the alkaline conditions. Ultimately, the recalcitrance of xylan must be dictated not only by the molecular structure of the xylan but also by its association with lignin or interaction with cellulose.

An interesting feature of the OLIMP spectra is the relative intensities corresponding to even or odd spacing of MeGlcpA. In S6, the ESI-MS signal intensities decrease gradually between X_6U and $X_{12}U$. However, in the other xylans, the even and odd patterns appear as two distinct series, where the even pattern is more common. Previously, similar preference for evenly spaced glucuronidation for X_nOs with $n > 5$ has been reported for *Arabidopsis* (Bromley et al., 2013; Grantham et al., 2017) while birch (Martínez-Abad et al., 2018) and aspen (Sivan et al., 2024) showed gradual decrease, as in S6 here. Other reports on Eucalyptus are from the production of XOs by hydrothermal treatment (Gullón et al., 2011; Kabel, 2002; Kabel et al., 2002), and not by controlled enzymatic hydrolysis. Therefore, the unspecific hydrolysis of the xylan yielded no distinct even pattern of MeGlcpA substitution. Even spacing of MeGlcpA has been shown to favour the interaction of xylan with cellulose (Busse-Wicher et al., 2014; Grantham et al., 2017), which

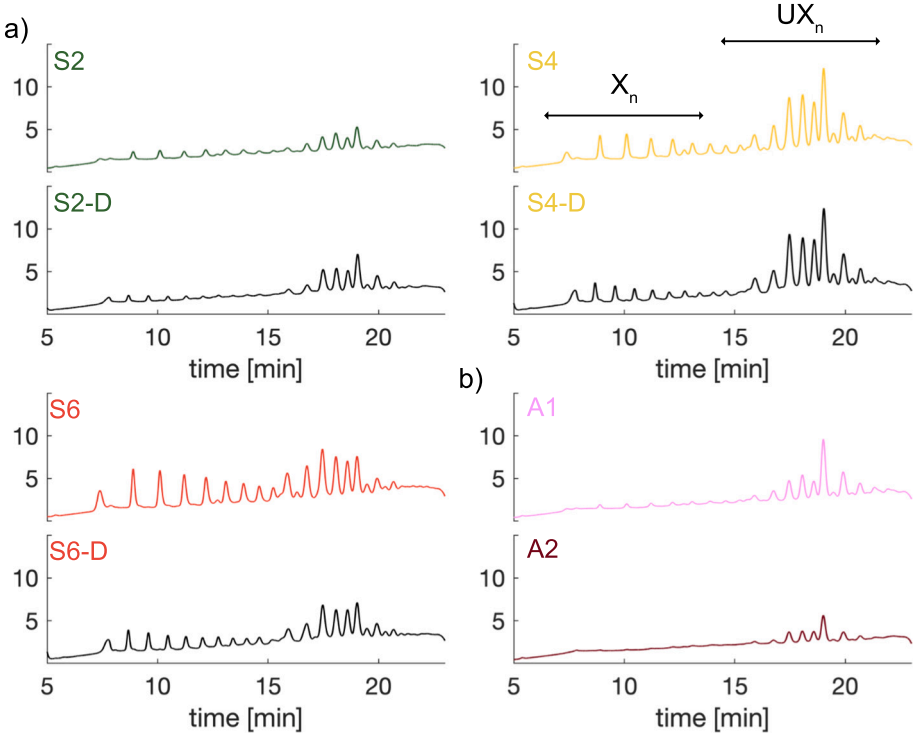

Fig. 3. Enzymatic hydrolysis of the extracts using GH30 glucuronoxylanase: Separation of the oligosaccharides by Ion-exchange chromatography. a) SWE extracts. Unmodified extract (coloured line) and deacetylated extract (black line) b) Alkali extracts.

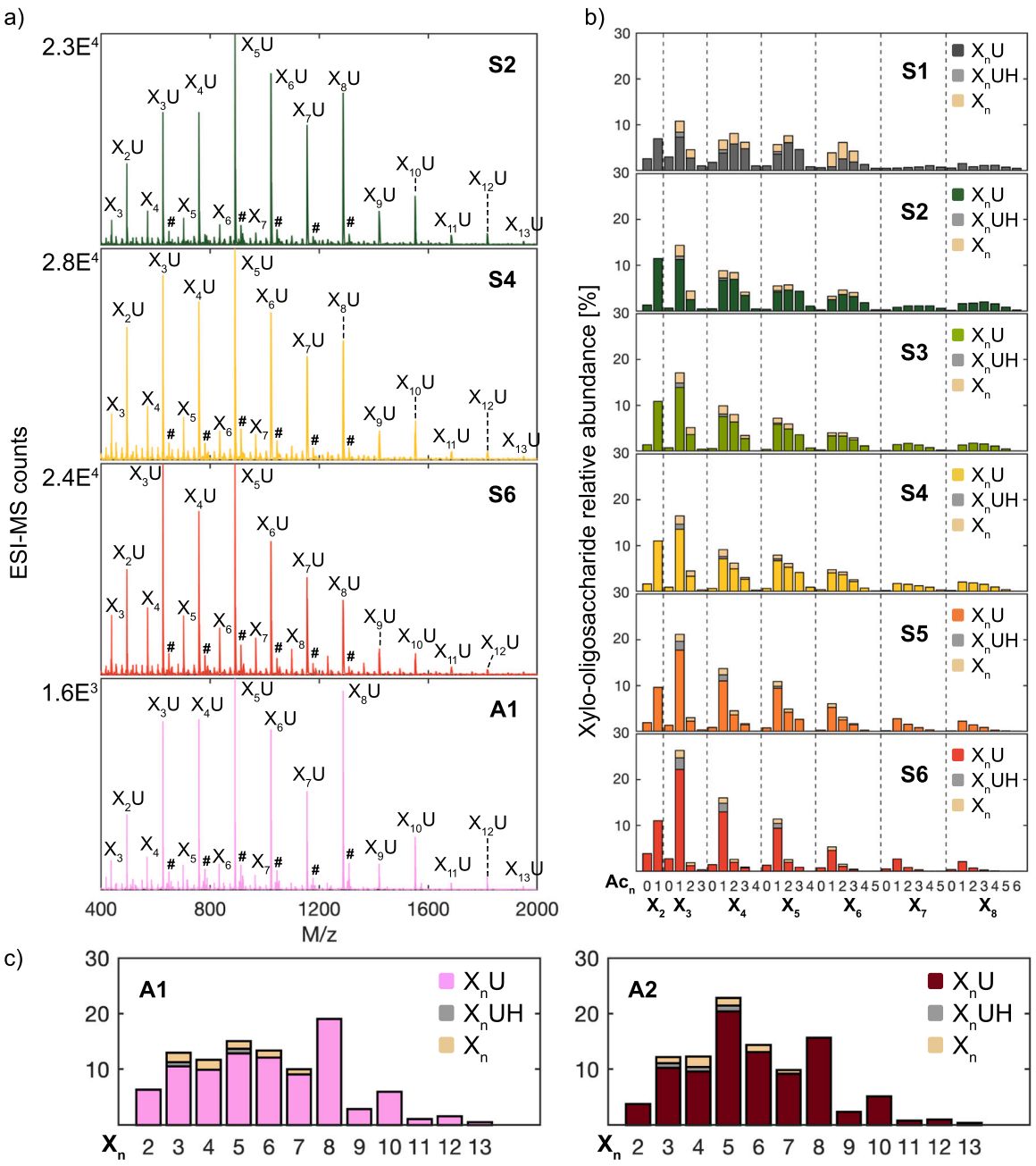

Fig. 4. Oligomeric mass profiling (OLIMP) of the extracted glucuronoxylan using GH30 endoxylanase. a) Electrospray mass spectrometry (ESI-MS) profiles of the deacetylated extracts. The hash (#) denotes a double sodium adduct. b) Relative abundance of oligosaccharides based on ESI-MS counts of duplicate digestions. c) Relative abundance of oligosaccharides in the alkaline extracts. A1 from the KOH-step and A2 from the NaOH-step.

may explain why the recalcitrant xylan from the alkali extractions had pronounced even spacing of MeGlcpA. It is more difficult to explain why the S1-S3 fraction also had even spacing on $X_{6\text{-}12}U$ solely based on interactions between cell wall polymers. Here the microscopic structure of the wood and the mass transport from different cell wall layers and types of cells may play a role in xylan extractability.

3.2.2. *Eucalyptus GX contains even and consecutive patterns of acetylation*

Acetylation of the xylan was preserved during the SWE in buffered conditions. Fig. 4b shows the calculated relative abundances for 3 series of oligosaccharides with general formulae X_nUAc_n, X_nAc_n and X_nUHAc_n, where the hexose is a galactosyl unit. The ESI-MS spectra of the GH30 digested extracts S1-S6 are shown in the supplementary Figs. S6-S7. The main series of XOs is X_nUAc_n that carries a single uronic acid group. In general, Fig. 4b shows a highly complex pattern of acetylation present in *Eucalyptus* xylan. Considering the X_5U, the least recalcitrant xylans are highly acetylated, carrying typically double or triple acetylations. The proportion of single acetylation increases with the extraction time, which agrees with the decreasing DsAc calculated from the released acetic acid by saponification 1. Better digestibility of the deacetylated extracts as shown by the comparison of the HPLC-SEC chromatograms (Fig. S3) indicates the possibility of highly acetylated xylan segments that are not accessible to the GH30.

In an effort to elucidate the spacing of acetyl groups, we derivatised XOs produced by GH30 and separated them by HPLC. Here, we focused on the xylopentaoses (X_5UAc_n), which were the most abundant motifs in the initial MS spectra (OLIMP). To that end, single ion monitoring (SIM) of the derivatized XOs revealed one isomer for the X_5UAc_1 but three and

two isomers for the X_5UAc_2 and X_5UAc_3, respectively, indicating different acetyl positions on these motifs (Fig. 5). Fragmentation of the major motifs from SIM 1 and 6 showed that one acetyl group resides always on the same residue as MeGlcpA with characteristic Y-ions *m/z* 636 and 272 (X_2UAc_1 + AA-label and X_1 + AA-label). Additional ions of m/z 984 (X_4UAc_3 + AA-label) and 768 (X_3UAc_1 + AA-label) from the SIM 6 showed evenly placed acetyl groups with structure XX2ac + 3acXU3acX. Similarly, the even pattern was preferred for X_5UAc_2 (Fig. S8).

The minor motifs corresponding to the SIM 2 and 5 were found to represent consecutive acetylation. The characteristic fragments are 810 and 620 m/z, which are X_3Ac_2 with and without MeGlcpA. In addition, the presence of Y4-ion, corresponding to fragmentation at the 4th xylose position from the reducing end of the oligomer, with m/z 984 confirmed that the third acetyl group is not on the non-reducing end. Hence, minor motifs with structures $XXX^{2ac/3ac}U^{3ac}X$ and $XX^{2ac/3ac}X^{2ac/3ac}U^{3ac}X$ were proposed. From the fragmentation pattern is it not possible to decipher whether the xylose is 2-O or 3-O acetylated.

3.2.3. *Consecutive glucuronidation present in Eucalyptus xylan*

When S4 xylan was incubated with GH10 and derivatized, a small number of ions with m/z 1180 were detected by ESI-MS single ion monitoring (Fig. 6). The m/z 1180 matched with xylopentaose substituted with two MeGlcpA units. Indeed, the following fragmentation revealed a series of Y-ions carrying two (Y4), one (Y3) and no MeGlcpA (Y2, Y1) indicating a presence of structure $XU^{4m2}U^{4m2}XX$. Recently, consecutive glucuronidation has been detected in aspen (Sivan et al., 2024). This growing evidence of consecutive glucuronidation in angiosperms indicates a more complex pattern of substitution than previously known. Furthermore, this feature has been previously detected in softwood arabinoglucuronoxylan (Martínez-Abad et al., 2017, 2020), which shows that consecutive glucuronidation has been conserved among different tree species.

3.3. *Galactosylation alters the enzymatic degradability of Eucalyptus xylan*

The *Eucalyptus* xylan has been shown to carry terminal galactose substitutions on the glucuronic acid groups (Shatalov et al., 1999). Our xylan-rich SWE extracts contained a large amount of galactose and more than half of the MeGlcpA were galactosylated (Table 1). Surprisingly, we could find only a small amount of galactosylated XOs in the mass spectra

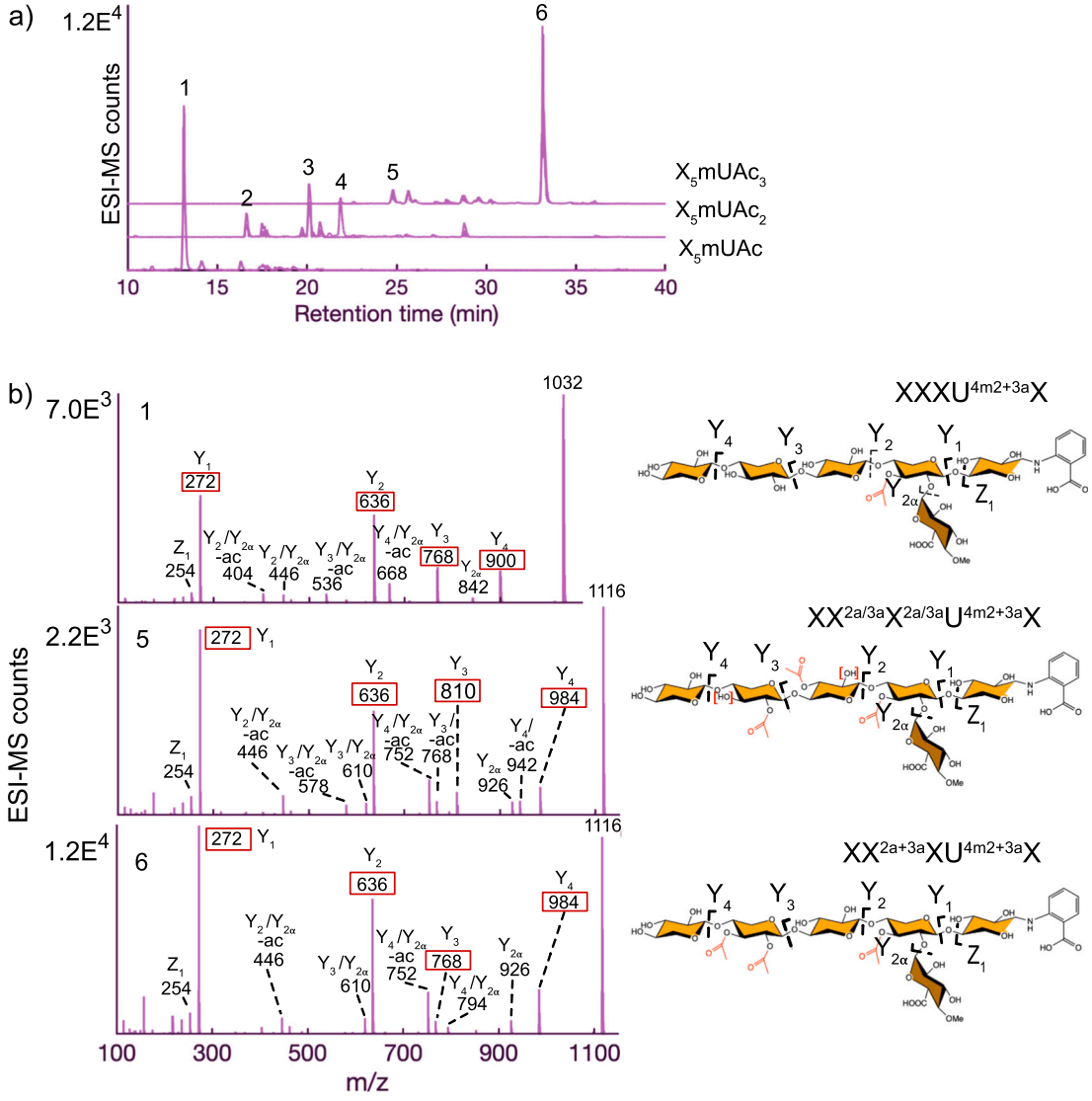

Fig. 5. Oligosaccharide sequencing of the S4 extract. a) Single ion monitoring (SIM) chromatograms of the UX_5Ac_n isomers. b) Fragmentation of the peaks 1,5 and 6 and assignation of the fragments according to the nomenclature proposed by Domon and Costello (1988). Proposed structures based on the fragmentation and nomenclature according to Fauré et al. (2009).

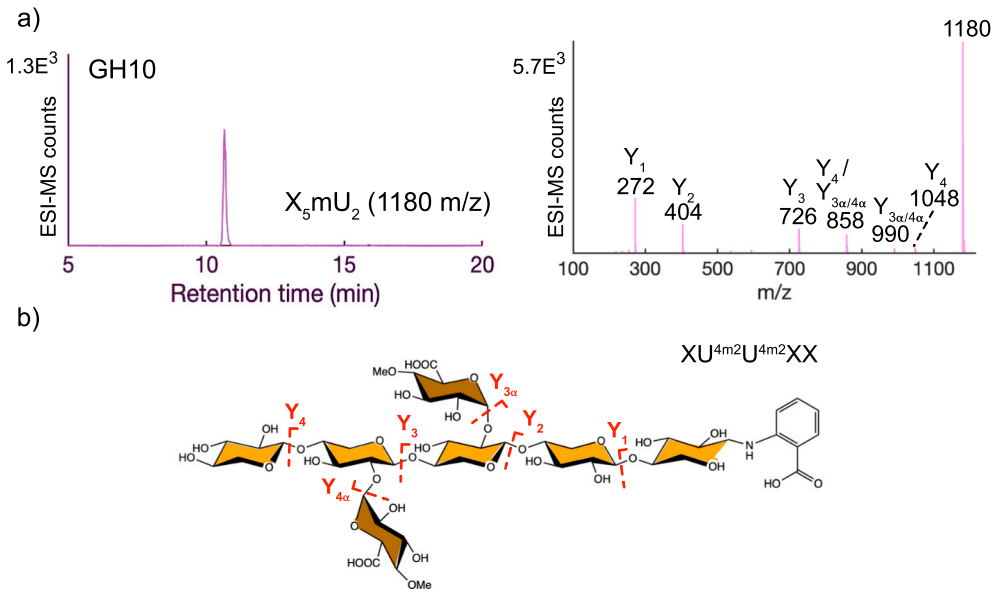

Fig. 6. Oligosaccharide sequencing after incubation with GH10 endoxylanase. a) Single ion monitoring (SIM) chromatogram. Fragmentation of the m/z 1180 ion and assignation of the fragments according to the nomenclature proposed by Domon and Costello (1988). b) Proposed structure based on the fragmentation and nomenclature according to Fauré et al. (2009).

of the extracts digested by GH30 glucuronoxylanase. According to Linares-Pasten et al. (2017) docking of GH30 near the MeGlcpA is characterized by a change of xylan conformation from a 3-fold to a bend. It may be that the terminal galactose hinders this conformational adaptation. Even though the majority of GH30 glucuronoxylanases do not tolerate substitutions on the MeGlcpA, a recent study by Yu et al. (2024) showed that there exists GH30 that have altered structurally to accommodate more complex side groups. To this end, docking studies are needed to explore how the structural change affects the conformation of xylan upon interaction with different types of GH30.

To assess whether there is galactose attached to xylan, as the monosaccharide analysis indicates, we decided to incubate two xylan-rich samples, S4 and A1, using a GH36 α-galactosidase. No galactose was detected by ion chromatography (Fig. 7a) despite repeated trials. A literature search revealed an interesting possibility, Togashi et al. (2009) suggested that the anomeric form of galactose in Eucalyptus would be a β instead of an α. To examine this possibility, we incubated the S4 and A1 extracts with a β-galactosidase (GH35), which indeed released a significant amount of galactose from both an SWE (S4) and alkali-extracted xylan (A1) (Fig. 7a). This confirms that the MeGlcpA of Eucalyptus xylan is indeed substituted by β-1 → 2-D-galactopyranose and not α-1 → 2-D-galactopyranose as commonly thought. Recently, Yu et al. (2024) showed a similar effect by using a β-galactosidase.

Parallel to the work with the galactosidases, we incubated the S4 and A1 samples using GH10 which does not require MeGlcpA substitution for xylan hydrolysis. Now, in addition to the usual UXOs, a series of hexoses containing XOs appeared (Fig. 7c). We detected X_nUH ($n = 3$–5) in the A1 and X_nUHAc_n ($n = 2$–4, Acn = 0–3) in the S4. X_3UHAc_1 was the 3rd largest signal in the S4 after the X_3UAc_1 and X_3Ac_1, showing the xylan indeed contains a significant amount of galactose.

An aliquot of galactosylated oligosaccharides from GH10 incubation was labelled with anthranilic acid (AA) and fragmented for determination of the positions of Gal*p*, MeGlcpA and acetyl (Fig. 8). The main motifs corresponding to the SIM 3–4 showed that the acetyl group is on the same xylopyranosyl residues as the Galp-MeGlcpA substitution, similar to the UXOs without a galactopyranosyl unit (Fig. 5). Generally, the Galp-MeGlcpA substitution was placed at the −2 or − 3 position. Previous reports note that GH10 tolerates acidic substitution (MeGlcpA) at −3 Biely et al., 2013) and + 1 subsites (Biely et al., 2013; Pollet et al., 2010), whereas Ara*f* is tolerated at −2 (Linares-Pasten et al., 2017; Rudjito et al., 2023). Our results indicate that addition of neutral substitution to the MeGlcpA allows the xylan backbone to be cleaved closer to the substitution on the aglycone side. Furthermore, the smallest motif (SIM 1, Fig. S9) had the Galp-MeGlcpA on the reducing end of xylosyl. Since it is reported to be a banned position regarding enzymatic hydrolysis (Biely et al., 2013), it was thought these fragments originate from the reducing end of the xylan polymers.

The large difference in the amount of galactosylated UXOs from GH10 and GH30 incubations indicates that the Galp-MeGlcpA motifs are clustered on the xylan. If they were evenly distributed, we would have expected to detect XOs with one MeGlcpA (reducing end) and one Galp-MeGlcpA (closer to non-reducing end) after a GH30 incubation. However, such XOs were absent in the samples.

3.4. *Proposed supramolecular organization of the hemicellulose populations in Eucalyptus cell walls*

The wood of *Eucalyptus* contains 15–23 % glucuronoxylan and 1–4 % glucomannan (Carvalho, 2015; Willför et al., 2005). We have thoroughly studied the molecular structure of *Eucalyptus* glucuronoxylan, which was extracted under sequential subcritical water and alkaline conditions, using mass spectrometric approaches. The use of specific xylanolytic enzymes for the selective deconstruction of the xylan structure into amenable oligosaccharides for sequencing has revealed a complex intramolecular substitution pattern in terms of glucuronidation, galactosylation and acetylation. General molecular features of water and alkali-extracted xylans and the cleavage sites by GH30 and GH10 are illustrated in Fig. 9a. These intramolecular motifs play a role in the interaction with cellulose microfibrils and lignin and therefore modulate the supramolecular architecture in secondary cell walls. The possible organization of the xylan with different motifs in the Eucalyptus secondary cell wall is presented in Fig. 9b. We have shown that the Eucalyptus xylan contains major motifs of i) sparse and even glucuronidation, ii) tight and odd glucuronidation with high acetylation iii) aggregated Galp-MeGlcpA that are not hydrolyzed by GH30. Generally, odd spacing is favoured on fragments X_nUAc_n with $X_{n<5}$, whereas even spacing is favoured on X_nUAc_n with $X_{n>5}$, which agrees with the mode of action of the GUX enzymes that add the mGlcA decorations during xylan synthesis (Bromley et al., 2013). Even spacing of acetylation is more common than odd on $X_5UAc_{2–3}$.

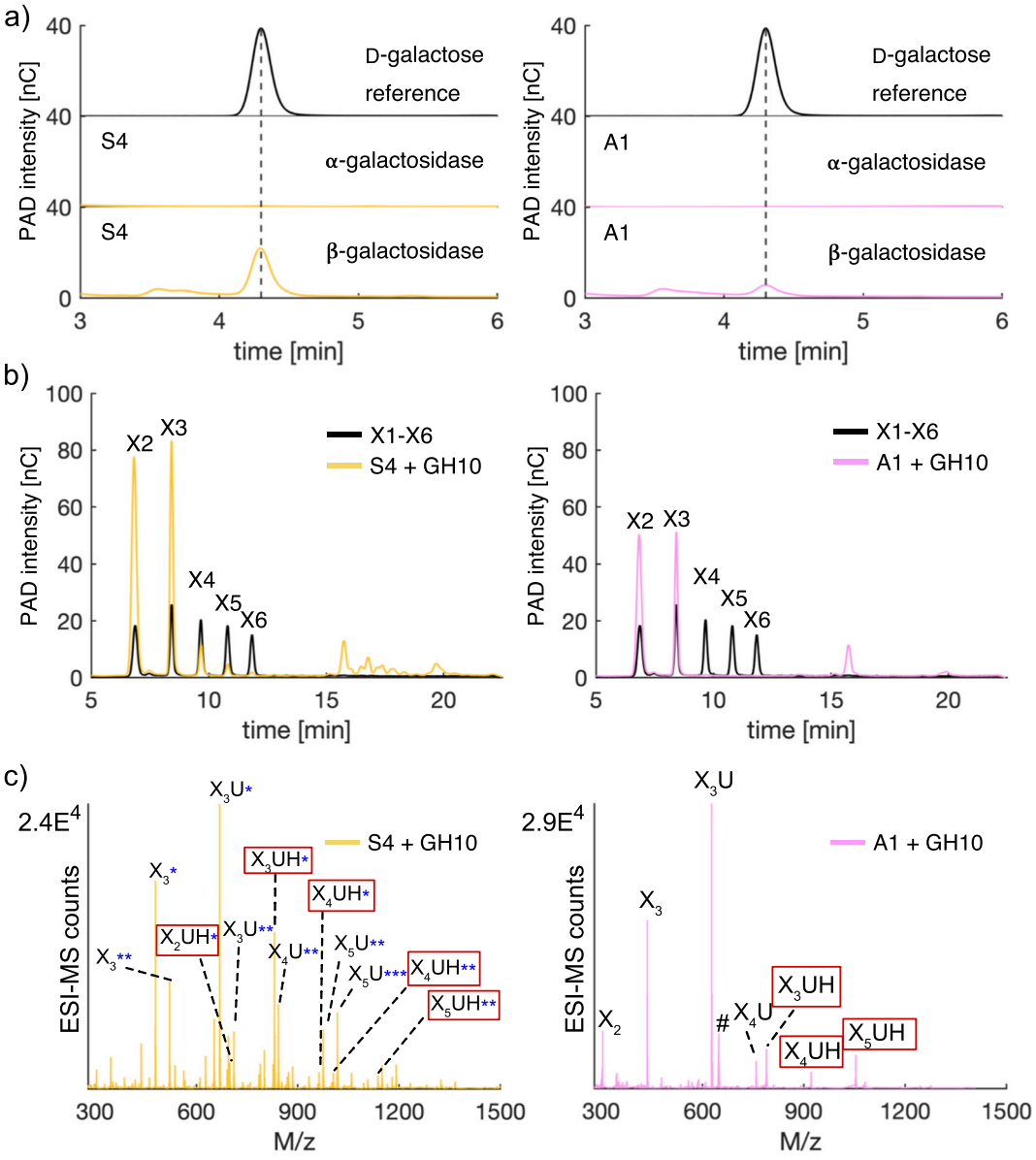

Fig. 7. a) Quantification of the released galactose by enzymatic hydrolysis of xylan. Ion-exchange chromatography of the galactose standard and the extracts digested by α-galactosidase (GH36) or β-galactosidase (GH35). The line indicates the elution time (4.30 min) of the galactose standard. b) Xylo-oligosaccharide standards (black line) and the GH10 digested extracts (coloured line) separated by Ion-Exchange Chromatography c) Electrospray mass spectrometry (ESI-MS) profiles of the xylo-oligosaccharides from GH10 digestion. Blue asterisks indicate the number of acetyl groups, the hash (#) denotes a double sodium adduct and the galactosylated xylo-oligosaccharides are highlighted. Complete assignments of the sample S4 in supplementary Fig. 10.

In this regard, evenly spaced MeGlcpA substitutions allow close association of xylan with cellulose (Busse-Wicher et al., 2014; Martínez-Abad et al., 2017; Simmons et al., 2016), while odd-spacing with lignin (Simmons et al., 2016) through covalent linkages (Giummarella et al., 2019). Furthermore, a higher degree of acetylation and glucuronidation improves the solubility of xylan, and the presence of both tight and sparse pattern substitution within the same polymer could improve the xylan-mediated interactions between cellulose and lignin within the cell wall. The MeGlcpA substitutions could also promote xylan-xylan interactions via metal cation bridges (Pereira et al., 2017). In *Eucalyptus*, the galactosylation adds a non-acidic substitution on the xylan backbone, which has been suggested to link to pectin (Shatalov et al., 1999). If this is true, the galactosylated xylan would be expected to be concentrated in the S1-layer of the secondary cell wall, adjacent to the primary cell wall.

4. Conclusions

Multiple patterns of substitution in *Eucalyptus* xylans were identified: preferential even glucuronidation on xylo-oligosaccharides with degree of polymerization between 6 and 12, major motifs of even acetylation and minor motifs of odd acetylation. In galactosylated XOs, acetylation was shown to be on the same xylosyl as the Galp-MeGlcpA substitution and the release of galactose from xylan by β-galactosidase indicated that the terminal galactose has β- and not α-anomer as originally thought. In addition, galactosylation of MeGlcpA was shown to hinder the hydrolysis by GH30. Furthermore, the structure-recalcitrance relationship of *Eucalyptus* xylan was proved as a complex matter. Oligomeric mass profiling revealed that even and odd glucuronidation occurs in both water and alkali extractable fractions. Finally, the majority of the hardwood glucomannan was resistant to extraction with water, which may be explained by its close association with cellulose and/or lignin as

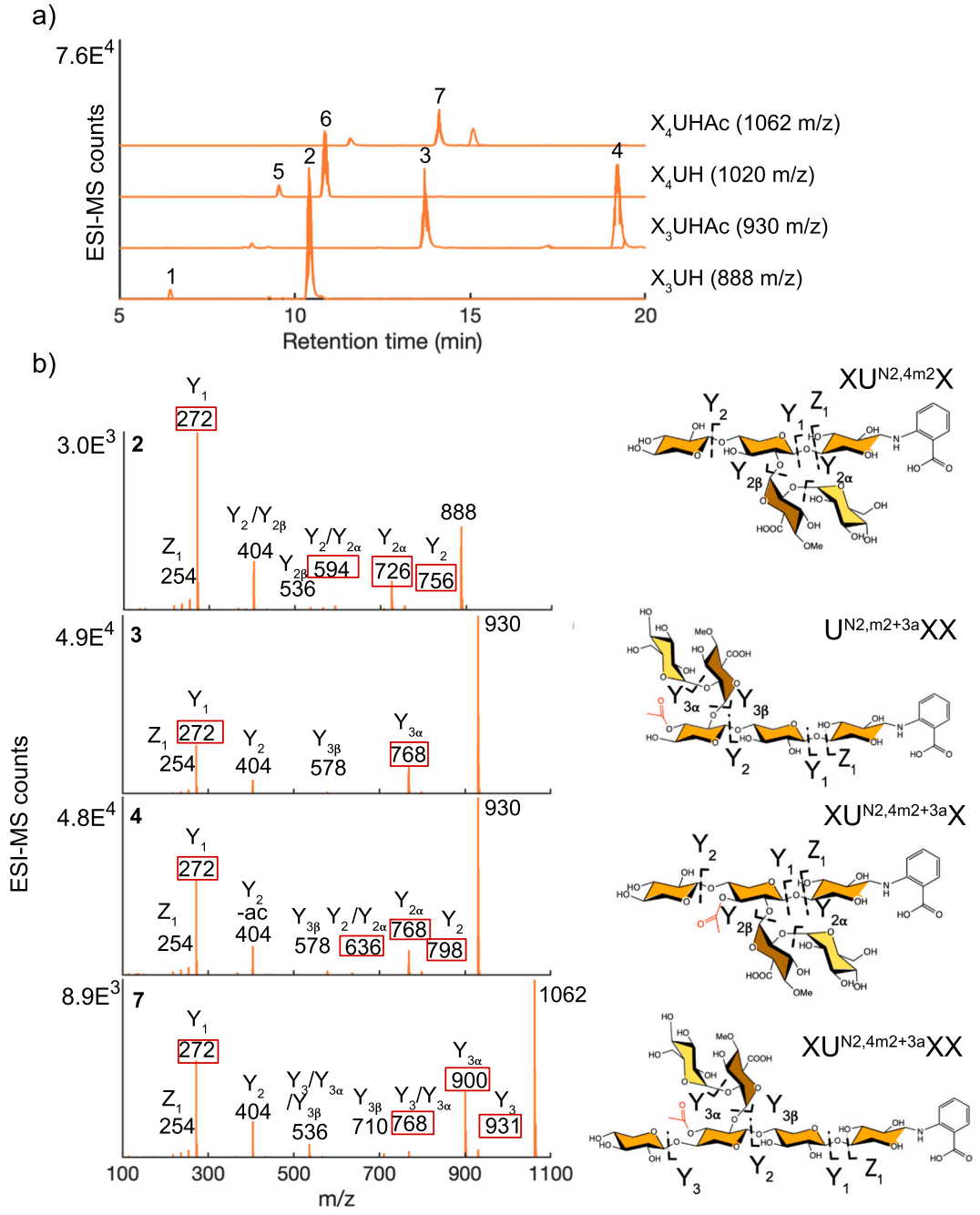

Fig. 8. Oligosaccharide sequencing after incubation with GH10 endoxylanase. a) Single ion monitoring (SIM) chromatograms. b) Fragmentation of the peaks numbered on the SIM for peaks 1,5 and 6 and assignation of the fragments according to the nomenclature proposed by Domon and Costello (1988). See Supplementary Fig. S8 for SIM 2,3 and 4. Proposed structures based on the fragmentation and nomenclature according to Fauré et al. (2009).

well as its localization within the cell wall (Handford et al., 2003). These findings deepen our understanding of the structure of xylan from *Eucalyptus*, which is a globally important source of wood biomass. Furthermore, comparison of tree species from different orders such as *Eucalyptus* (Myrtales), birch (Fagales) and aspen (Malpighiales) allows us to evaluate which structural aspects of the hemicelluloses are widely spread over the planta, and which perhaps more specific responses to the habitat and a result of later evolutionary adaptations. Such structural differences may have important implications for the interaction of xylan with cellulose and lignin, the separation of the wood hemicelluloses for industrial use and the properties of the hemicellulose-based materials.

CRediT authorship contribution statement

Emilia Heinonen: Writing – review & editing, Writing – original draft, Visualization, Methodology, Investigation, Formal analysis, Data curation, Conceptualization. **Pramod Sivan:** Writing – review & editing, Methodology, Investigation. **Amparo Jiménez-Quero:** Writing – review & editing, Methodology, Investigation. **Mikael E. Lindström:** Writing – review & editing, Supervision, Investigation. **Jakob Wohlert:** Writing – review & editing, Supervision, Investigation. **Gunnar Henriksson:** Writing – review & editing, Supervision, Investigation. **Francisco Vilaplana:** Writing – review & editing, Supervision, Resources, Project administration, Funding acquisition, Conceptualization.

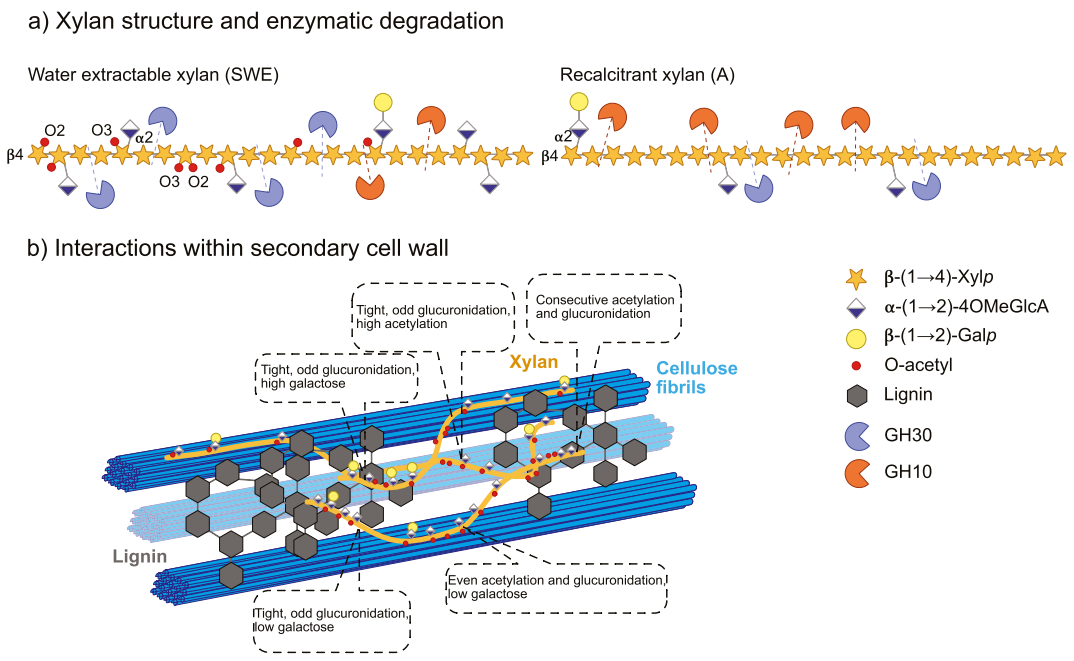

Fig. 9. Glucuronoxylan from *Eucalyptus* wood, schematic structure a) Structural diversity of molecular motifs and degradation susceptibility by GH30 and GH10 endoxylanases. SWE = subcritical water extraction, A = alkaline extraction. b) Proposed model of secondary cell wall showing molecular interactions of GX motifs with cellulose and lignin.

Declaration of competing interest

The authors declare the following financial interests/personal relationships which may be considered as potential competing interests: Francisco Vilaplana reports financial support was provided by Knut and Alice Wallenberg Foundation. Francisco Vilaplana reports financial support was provided by Swedish Research Council. Francisco Vilaplana reports a relationship with Oatly AB that includes: employment. Francisco Vilaplana reports a relationship with Arla Foods amba that includes: board membership. If there are other authors, they declare that they have no known competing financial interests or personal relationships that could have appeared to influence the work reported in this paper.

Acknowledgements

This work was supported by the Knut and Alice Wallenberg Foundation through the Wallenberg Wood Science Centre; The Swedish Research Council (VR) [grant number 2020-04720] (F.V.).

Appendix A. Supplementary data

Supplementary data to this article can be found online at https://doi.org/10.1016/j.carbpol.2025.123246.

Data availability

Data will be made available on request.

References

Alonso, J. L., Domínguez, H., Parajó, J. C., & Vázquez, M. J. (2002). Enzymatic processing of crude xylooligomer solutions obtained by autohydrolysis of eucalyptus wood. *Food Biotechnology, 16*(2), 91–105. https://doi.org/10.1081/fbt-120014321. January.

Biely, P., Cziszárová, M., Uhliariková, I., Agger, J. W., Li, X.-L., Eijsink, V. G., & Westereng, B. (2013). Mode of action of acetylxylan esterases on acetyl glucuronoxylan and acetylated oligosaccharides generated by a gh10 endoxylanase. *Biochimica et Biophysica Acta (BBA) - General Subjects, 1830*(11), 5075–5086. https://doi.org/10.1016/j.bbagen.2013.07.018. November.

Bromley, J. R., Busse-Wicher, M., Tryfona, T., Mortimer, J. C., Zhang, Z., Brown, D. M., & Dupree, P. (2013). GUX1 and GUX2 glucuronyltransferases decorate distinct domains of glucuronoxylan with different substitution patterns. *The Plant Journal, 74*(3), 423–434. https://doi.org/10.1111/tpj.12135. March.

Busse-Wicher, M., Gomes, T. C. F., Tryfona, T., Nikolovski, N., Stott, K., Grantham, N. J., … Dupree, P. (2014). The pattern of xylan acetylation suggests xylan may interact with cellulose microfibrils as a twofold helical screw in the secondary plant cell wall of arabidopsis thaliana. *The Plant Journal, 79*(3), 492–506. https://doi.org/10.1111/tpj.12575. July.

Carvalho, D. (2015). *Study on the structure and properties of xylan extracted from eucalyptus, sugarcane bagasse and sugarcane straw (no. 2015:59). (QC 20151023)*.

Chong, S.-L., Virkki, L., Maaheimo, H., Juvonen, M., Derba-Maceluch, M., Koutaniemi, S., … Tenkanen, M. (2014). O-acetylation of glucuronoxylan in arabidopsis thaliana wild type and its change in xylan biosynthesis mutants. *Glycobiology, 24*(6), 494–506. https://doi.org/10.1093/glycob/cwu017. , March.

Corradini, F. A., Baldez, T. O., Milessi, T. S., Tardioli, P. W., Ferreira, A. G., de Campos Giordano, R., & de L.C. Giordano, R.. (2018). Eucalyptus xylan: An in-houseproduced substrate for xylanase evaluation to substitute birchwood xylan. *Carbohydrate Polymers, 197*, 167–173. https://doi.org/10.1016/j.carbpol.2018.05.088. October.

Domon, B., & Costello, C. E. (1988). A systematic nomenclature for carbohydrate fragmentations in fab-ms/ms spectra of glycoconjugates. *Glycoconjugate Journal, 5*(4), 397–409. https://doi.org/10.1007/bf01049915

Evtuguin, D., Tomás, J., Silva, A., & Neto, C. (2003). Characterization of an acetylated heteroxylan from eucalyptus globulus labill. *Carbohydrate Research, 338*(7), 597–604. https://doi.org/10.1016/s0008-6215(02)00529-3. March.

Fauré, R., Courtin, C. M., Delcour, J. A., Dumon, C., Faulds, C. B., Fincher, G. B., … O'Donohue, M. J. (2009). A brief and informationally rich naming system for oligosaccharide motifs of heteroxylans found in plant cell walls. *Australian Journal of Chemistry, 62*(6), 533. https://doi.org/10.1071/ch08458. June.

Garrote, G., Domínguez, H., & Parajó, J. C. (2001). Study on the deacetylation of hemicelluloses during the hydrothermal processing of eucalyptus wood. *Holz als Roh- und Werkstoff, 59*(1–2), 53–59. https://doi.org/10.1007/s001070050473. April.

Giummarella, N., Pu, Y., Ragauskas, A. J., & Lawoko, M. (2019). A critical review on the analysis of lignin carbohydrate bonds. *Green Chemistry, 21*(7), 1573–1595. https://doi.org/10.1039/c8gc03606c

Gomes, T. M., de Sousa, A. P. M., Belenkiy, Y. I., & Evtuguin, D. V. (2020). Xylan accessibility of bleached eucalypt pulp in alkaline solutions. *Holzforschung, 74*(2), 141–148. https://doi.org/10.1515/hf-2019-0023. February.

Grantham, N. J., Wurman-Rodrich, J., Terrett, O. M., Lyczakowski, J. J., Stott, K., Iuga, D., … Dupree, P. (2017). An even pattern of xylan substitution is critical for interaction with cellulose in plant cell walls. *Nature Plants, 3*(11), 859–865. https://doi.org/10.1038/s41477-017-0030-8. October.

Gullón, P., González-Muñoz, M. J., Gool, M. P.v., Schols, H. A., Hirsch, J., Ebringerová, A., & Parajó, J. C. (2011). Structural features and properties of soluble products derived from eucalyptus globulus hemicelluloses. *Food Chemistry, 127*(4), 1798–1807. https://doi.org/10.1016/j.foodchem.2011.02.066. August.

Handford, M. G., Baldwin, T. C., Goubet, F., Prime, T. A., Miles, J., Yu, X., & Dupree, P. (2003). Localisation and characterisation of cell wall mannan polysaccharides in arabidopsis thaliana. *Planta, 218*(1), 27–36. https://doi.org/10.1007/s00425-003-1073-9. , November.

Hurlbert, J. C., & Preston, J. F. (2001). Functional characterization of a novel xylanase from a corn strain of Erwinia chrysanthemi. *Journal of Bacteriology, 183*(6), 2093–2100. https://doi.org/10.1128/jb.183.6.2093-2100.2001. March.

Kabel, M. (2002). Hydrothermally treated xylan rich by-products yield different classes of xylo-oligosaccharides. *Carbohydrate Polymers, 50*(1), 47–56. https://doi.org/10.1016/s0144-8617(02)00045-0. , October.

Kabel, M., Schols, H., & Voragen, A. (2002). Complex xylo-oligosaccharides identified from hydrothermally treated eucalyptus wood and brewery's spent grain. *Carbohydrate Polymers, 50*(2), 191–200. https://doi.org/10.1016/s0144-8617(02)00022-x. November.

Leppänen, K., Spetz, P., Pranovich, A., Hartonen, K., Kitunen, V., & Ilvesniemi, H. (2010). Pressurized hot water extraction of Norway spruce hemicelluloses using a flowthrough system. *Wood Science and Technology, 45*(2), 223–236. https://doi.org/10.1007/s00226-010-0320-z. March.

Linares-Pasten, J. A., Aronsson, A., & Karlsson, E. N. (2017). Structural considerations on the use of endo-xylanases for the production of prebiotic xylooligosaccharides from biomass. *Current Protein & Peptide Science, 19*(1). https://doi.org/10.2174/1389203717666160923155209. November.

Lisboa, S., Evtuguin, D., Neto, C. P., & Goodfellow, B. (2005). Isolation and structural characterization of polysaccharides dissolved in eucalyptus globulus Kraft black liquors. *Carbohydrate Polymers, 60*(1), 77–85. https://doi.org/10.1016/j.carbpol.2004.11.024. April.

Magaton, A. S., Silva, T. C. F., Colodette, J. L., Piló-Veloso, D., Milagres, F. R., & Resende, J. O. (2012). Behavior of xylans from the eucalyptus species. Part 2. Characterization of 4-o-methylglucuronoxylans isolated from black liquors of Kraft pulping of eucalyptus grandis and e. urophylla. *Holzforschung, 67*(2), 123–128. https://doi.org/10.1515/hf-2012-0035. September.

Martínez-Abad, A., Giummarella, N., Lawoko, M., & Vilaplana, F. (2018). Differences in extractability under subcritical water reveal interconnected hemicellulose and lignin recalcitrance in birch hardwoods. *Green Chemistry, 20*(11), 2534–2546. https://doi.org/10.1039/c8gc00385h

Martínez-Abad, A., Jiménez-Quero, A., Wohlert, J., & Vilaplana, F. (2020). Influence of the molecular motifs of mannan and xylan populations on their recalcitrance and organization in spruce softwoods. *Green Chemistry, 22*(12), 3956–3970. https://doi.org/10.1039/d0gc01207f

Martínez-Abad, A., Berglund, J., Toriz, G., Gatenholm, P., Henriksson, G., Lindström, M., … Vilaplana, F. (2017). Regular motifs in xylan modulate molecular flexibility and interactions with cellulose surfaces. *Plant Physiology, 175*(4), 1579–1592. https://doi.org/10.1104/pp.17.01184. October.

McKee, L. S., Sunner, H., Anasontzis, G. E., Toriz, G., Gatenholm, P., Bulone, V., … Olsson, L. (2016). A GH115 α-glucuronidase from schizophyllum commune contributes to the synergistic enzymatic deconstruction of softwood glucuronoarabinoxylan. *Biotechnology for Biofuels, 9*(1). https://doi.org/10.1186/s13068-015-0417-6. January.

Mian, A. J., & Timell, T. E. (1960). Isolation and properties of a glucomannan from the wood of red maple (acer rubrum l.). *Canadian Journal of Chemistry, 38*(9), 1511–1517. https://doi.org/10.1139/v60-211. September.

Pereira, C. S., Silveira, R. L., Dupree, P., & Skaf, M. S. (2017). Effects of xylan side-chain substitutions on xylan–cellulose interactions and implications for thermal pretreatment of cellulosic biomass. *Biomacromolecules, 18*(4), 1311–1321. https://doi.org/10.1021/acs.biomac.7b00067. March.

Pollet, A., Delcour, J. A., & Courtin, C. M. (2010). Structural determinants of the substrate specificities of xylanases from different glycoside hydrolase families. *Critical Reviews in Biotechnology, 30*(3), 176–191. https://doi.org/10.3109/07388551003645599. March.

Rudjito, R. C., Jiménez-Quero, A., Muñoz, M. D. C. C., Kuil, T., Olsson, L., Stringer, M. A., … Vilaplana, F. (2023). Arabinoxylan source and xylanase specificity influence the production of oligosaccharides with prebiotic potential. *Carbohydrate Polymers, 320*, 121233. https://doi.org/10.1016/j.carbpol.2023.121233. November.

Scott, R. W. (1989). Influence of cations and borate on the alkaline extraction of xylan and glucomannan from pine pulps. *Journal of Applied Polymer Science, 38*(5), 907–914. https://doi.org/10.1002/app.1989.070380512. , September.

Shatalov, A. A., Evtuguin, D. V., & Neto, C. P. (1999). (2-o-α-d-galactopyranosyl-4-o-methyl-α-d-glucurono)-d-xylan from eucalyptus globulus labill. *Carbohydrate Research, 320*(1–2), 93–99. https://doi.org/10.1016/s0008-6215(99)00136-6. July.

Simmons, T. J., Mortimer, J. C., Bernardinelli, O. D., Pöppler, A.-C., Brown, S. P., deAzevedo, E. R., … Dupree, P. (2016). Folding of xylan onto cellulose fibrils in plant cell walls revealed by solid-state NMR. *Nature Communications, 7*(1). https://doi.org/10.1038/ncomms13902. , December.

Sivan, P., Heinonen, E., Escudero, L., Gandla, M. L., Jiménez-Quero, A., Jönsson, L. J., … Vilaplana, F. (2024). Unraveling the unique structural motifs of glucuronoxylan from hybrid aspen wood. *Carbohydrate Polymers, 343*, 122434. https://doi.org/10.1016/j.carbpol.2024.122434. November.

Sivan, P., Heinonen, E., Latha Gandla, M., Jiménez-Quero, A., Özeren, H. D., Jönsson, L. J., … Vilaplana, F. (2023). Sequential extraction of hemicelluloses by subcritical water improves saccharification of hybrid aspen wood grown in greenhouse and field conditions. *Green Chemistry, 25*(14), 5634–5646. https://doi.org/10.1039/d3gc01020a

Sixta, H. (Ed.). (2006). *Handbook of pulp*. Weinheim: Wiley. https://doi.org/10.1002/9783527619887 (Mode of access: World Wide Web. System requirements: Web browser. Title from title screen (viewed on Mar. 27, 2008). Access may be restricted to users at subscribing institutions.).

Sjöström, E. (1993). *Wood chemistry* (Second edition ed.). San Diego: Elsevier. https://doi.org/10.1016/c2009-0-03289-9

Teleman, A., Nordström, M., Tenkanen, M., Jacobs, A., & Dahlman, O. (2003). Isolation and characterization of o-acetylated glucomannans from aspen and birch wood. *Carbohydrate Research, 338*(6), 525–534. https://doi.org/10.1016/s0008-6215(02)00491-3. , March.

Timell, T. (1961). Isolation of galactoglucomannans from the wood of gymnosperms. *TAPPI, 44*, 88–96.

Timell, T. (1964). Wood hemicelluloses: Part I. *Advances in Carbohydrate Chemistry, 19*, 247–302. https://doi.org/10.1016/s0096-5332(08)60284-2

Timell, T. (1965). Wood hemicelluloses: Part ii. *Advances in Carbohydrate Chemistry, 20*, 409–483. https://doi.org/10.1016/s0096-5332(08)60304-5

Togashi, H., Kato, A., & Shimizu, K. (2009). Enzymatically derived aldouronic acids from eucalyptus globulus glucuronoxylan. *Carbohydrate Polymers, 78*(2), 247–252. https://doi.org/10.1016/j.carbpol.2009.03.035. September.

Willför, S., Sundberg, A., Pranovich, A., & Holmbom, B. (2005). Polysaccharides in some industrially important hardwood species. *Wood Science and Technology, 39*(8), 601–617. https://doi.org/10.1007/s00226-005-0039-4. October.

Xu, C., Leppänen, A.-S., Eklund, P., Holmlund, P., Sjöholm, R., Sundberg, K., & Willför, S. (2010). Acetylation and characterization of spruce (picea abies) galactoglucomannans. *Carbohydrate Research, 345*(6), 810–816. https://doi.org/10.1016/j.carres.2010.01.007. April.

Yu, L., Wilson, L. F. L., Terrett, O. M., Wurman-Rodrich, J., Łyczakowski, J. J., Yu, X., … Dupree, P. (2024). Evolution of glucuronoxylan side chain variability in vascular plants and the compensatory adaptations of cell wall–degrading hydrolases. *New Phytologist*. https://doi.org/10.1111/nph.19957. July.